発表者氏名	論文タイトル名	発表誌名	巻号	ページ	出版年
Sawada T, Minamino T, Fu HY, Asai M, Okuda K, Isomura T, Yamazaki S, Asano Y, Okada K, Tsukamoto O, Sanada S, Asanuma H, Asakura M, Takashima S, Kitakaze M, Komuro I	X-box binding protein 1 regulates brain natriuretic peptide through a novel AP1/CRE-like element in cardiomyocytes.	*J Mol Cell Cardiol.*	48	1280-1289	2010
Naito AT, Okada S, Minamino T, Iwanaga K, Liu ML, Sumida T, Nomura S, Sahara N, Mizoroki T, Takashima A, Akazawa H, Nagai T, Shiojima I, Komuro I	Promotion of CHIP-mediated p53 degradation protects the heart from ischemic injury.	*Circ Res.*	106	1692-1702	2010
Sandoval JC, Nakagawa-Toyama Y, Masuda D, Tochino Y, Nakaoka H, Kawase R, Yuasa-Kawase M, Nakatani K, Inagaki M, Tsubakio-Yamamoto K, Ohama T, Nishida M, Ishigami M, Komuro I, Yamashita S	Fenofibrate reduces postprandial hypertriglyceridemia in CD36 knockout mice.	*J Atheroscler Thromb.*	17	610-618	2010

発表者氏名	論文タイトル名	発表誌名	巻号	ページ	出版年
Toko H, Takahashi H, Kayama Y, Okada S, Minamino T, Terasaki F, Kitaura Y, Komuro I	ATF6 is important under both pathological and physiological states in the heart.	*J Mol Cell Cardiol.*	49	113-120	2010
Taneike M, Yamaguchi O, Nakai A, Hikoso S, Takeda T, Mizote I, Oka T, Tamai T, Oyabu J, Murakawa T, Nishida K, Shimizu T, Hori M, Komuro I, Shirasawa T, Mizushima N, Otsu K	Inhibition of autophagy in the heart induces age-related cardiomyopathy.	*J Mol Cell Cardiol.*	6	600-606	2010
Fu HY, Okada K, Liao Y, Tsukamoto O, Isomura T, Asai M, Sawada T, Okuda K, Asano Y, Sanada S, Asanuma H, Asakura M, Takashima S, Komuro I, Kitakaze M, Minamino T	Ablation of C/EBP homologous protein attenuates endoplasmic reticulum-mediated apoptosis and cardiac dysfunction induced by pressure overload.	*Circulation*	122	361-369	2010

発表者氏名	論文タイトル名	発表誌名	巻号	ページ	出版年
Nakaoka Y, Shioyama W, Kunimoto S, Arita Y, Higuchi K, Yamamoto K, Fujio Y, Nishida K, Kuroda T, Hirota H, Yamauchi-Takihara K, Hirano T, Komuro I, Mochizuki N	SHP2 mediates gp130-dependent cardiomyocyte hypertrophy via negative regulation of skeletal alpha-actin gene.	*J Mol Cell Cardiol.*	49	157-164	2010
Toko H, Takahashi H, Kayama Y, Oka T, Minamino T, Okada S, Morimoto S, Zhan DY, Terasaki F, Anderson ME, Inoue M, Yao A, Nagai R, Kitaura Y, Sasaguri T, Komuro I	Ca^{2+}/calmodulin-dependent kinase IIδ causes heart failure by accumulation of p53 in dilated cardiomyopathy.	*Circulation*	122	891-899	2010
Sandoval JC, Nakagawa-Toyama Y, Masuda D, Tochino Y, Nakaoka H, Kawase R, Yuasa-Kawase M, Nakatani K, Inagaki M, Tsubakio-Yamamoto K, Ohama T, Matsuyama A, Nishida M, Ishigami M, Komuro I, Yamashita S	Molecular mechanisms of ezetimibe-induced attenuation of postprandial hypertriglyceridemia.	*J Atheroscler Thromb.*	17	914-924	2010

発表者氏名	論文タイトル名	発表誌名	巻号	ページ	出版年
Higo S, Asano Y, Kato H, Yamazaki S, Nakano A, Tsukamoto O, Seguchi O, Asai M, Asakura M, Asanuma H, Sanada S, Minamino T, Komuro I, Kitakaze M, Takashima S	Isoform-specific intermolecular disulfide bond formation of heterochromatin protein 1 (HP1).	*J Biol Chem.*	285	31337-31347	2010
Minamino T, Komuro I, Kitakaze M	Endoplasmic reticulum stress as a therapeutic target in cardiovascular disease.	*Circ Res.*	107	1071-1082	2010
Akazawa H, Yasuda N, Miura S, Komuro I	Assessment of inverse agonism for the angiotensin II type 1 receptor.	*Methods Enzymol.*	485	25-35	2010
Naito AT, Shiojima I, Komuro I	Wnt signaling and aging-related heart disorders.	*Circ Res.*	107	1295-1303	2010
Tokunaga M, Liu ML, Nagai T, Iwanaga K, Matsuura K, Takahashi T, Kanda M, Kondo N, Wang P, Naito AT, Komuro I	Implantation of cardiac progenitor cells using self-assembling peptide improves cardiac function after myocardial infarction.	*J Mol Cell Cardiol.*	49	972-983	2010
Li L, Zhou N, Gong H, Wu J, Lin L, Komuro I, Ge J, Zou Y	Comparison of angiotensin II type 1-receptor blockers to regress pressure overload-induced cardiac hypertrophy in mice.	*Hypertens Res.*	33	1289-1297	2010

発表者氏名	論文タイトル名	発表誌名	巻号	ページ	出版年
Aoki A, Ozaki K, Sato H, Takahashi A, Kubo M, Sakata Y, Onouchi Y, Kawaguchi T, Lin TH, Takano H, Yasutake M, Hsu PC, Ikegawa S, Kamatani N, Tsunoda T, Juo SH, Hori M, Komuro I, Mizuno K, Nakamura Y, Tanaka T	SNPs on chromosome 5p15.3 associated with myocardial infarction in Japanese population.	*J Hum Genet.*	56	47-51	2011
Ohno K, Amano Y, Kakuta H, Niimi T, Takakura S, Orita M, Miyata K, Sakashita H, Takeuchi M, Komuro I, Higaki J, Horiuchi M, Kim-Mitsuyama S, Mori Y, Morishita R, Yamagishi S	Unique "delta lock" structure of telmisartan is involved in its strongest binding affinity to angiotensin II type 1 receptor.	*Biochem Biophys Res Commun.*	404	434-437	2011
Akazawa H, Komuro I	Navigational error in the heart leads to premature ventricular excitation.	*J Clin Invest.*	121	513-516	2011
Sanada S, Komuro I	Costarring statins with ARBs: going to be a smash hit?	*Circ J.*	75	540-541	2011

発表者氏名	論文タイトル名	発表誌名	巻号	ページ	出版年
Ikeda H, Shiojima I, Oka T, Yoshida M, Maemura K, Walsh K, Igarashi T, Komuro I	Increased Akt-mTOR signaling in lung epithelium is associated with respiratory distress syndrome in mice.	*Mol Cell Biol.*	31	1054-1065	2011
Shioyama W, Nakaoka Y, Higuchi K, Minami T, Taniyama Y, Nishida K, Kidoya H, Sonobe T, Naito H, Arita Y, Hashimoto T, Kuroda T, Fujio Y, Shirai M, Takakura N, Morishita R, Yamauchi-Takihara K, Kodama T, Hirano T, Mochizuki N, Komuro I	Docking protein Gab1 is an essential component of postnatal angiogenesis after ischemia via HGF/c-met signaling.	*Circ Res.*	108	664-675	2011

Naunyn-Schmiedeberg's Arch Pharmacol (2008) 377:393–399
DOI 10.1007/s00210-007-0215-1

REVIEW

A novel mechanism of mechanical stress-induced angiotensin II type 1–receptor activation without the involvement of angiotensin II

Noritaka Yasuda · Hiroshi Akazawa · Yingjie Qin · Yunzeng Zou · Issei Komuro

Received: 10 August 2007 / Accepted: 31 October 2007 / Published online: 29 November 2007

Abstract The angiotensin II (AngII) type 1 (AT_1) receptor is a seven transmembrane-spanning G-protein-coupled receptor, and the activation of AT_1 receptor plays an important role in the development of load-induced cardiac hypertrophy. Locally generated AngII was believed to trigger cardiac hypertrophy by an autocrine or paracrine mechanism. However, we found that mechanical stress can activate AT_1 receptor independently of AngII. Without the involvement of AngII, mechanical stress not only activates extracellular signal-regulated kinases in vitro, but also induces cardiac hypertrophy in vivo. All of these events are inhibited by candesartan as an inverse agonist for AT_1 receptor. It is conceptually novel that AT_1 receptor directly mediates mechanical stress-induced cellular responses, and inverse-agonist activity emerges as an important pharmacological parameter for AT_1-receptor blockers that determines their efficacy in preventing organ damage in cardiovascular diseases.

N. Yasuda · H. Akazawa · Y. Qin · I. Komuro (✉)
Department of Cardiovascular Science and Medicine,
Chiba University Graduate School of Medicine,
1-8-1 Inohana, Chuo-ku,
Chiba 260-8670, Japan
e-mail: komuro-tky@umin.ac.jp

H. Akazawa
Division of Cardiovascular Pathophysiology,
Chiba University Graduate School of Medicine,
1-8-1 Inohana, Chuo-ku,
Chiba 260-8670, Japan

Y. Zou
Shanghai Institute of Cardiovascular Diseases,
Zhongshan Hospital, Fudan University,
180 Feng Lin Road,
Shanghai 200032, China

Keywords Angiotensin II type 1–receptor blocker · Conformational change · Inverse agonist · Mechanical stress

Introduction

Cardiac hypertrophy is one of the most important organ damages induced by pressure overload such as hypertension. Cardiac hypertrophy is not only an adaptive state that precedes heart failure, but also an independent risk factor for major cardiac events, such as ischemic heart disease, arrhythmia and sudden death (Levy et al. 1990). Therefore, it is important to elucidate the molecular mechanism underlying the development of cardiac hypertrophy. Many experimental studies have shown that various humoral factors such as vasoactive peptides, the sympathetic nervous system, cytokines and growth factors contribute to the development of cardiac hypertrophy. All components of the renin-angiotensin system such as angiotensinogen, renin, angiotensin-converting enzyme and angiotensin receptors have been identified in the heart (Baker et al. 1992; Lee et al. 1993). Angiotensin II (AngII) evokes hypertrophic responses such as protein synthesis and reprogramming of gene expression via AngII type 1 (AT_1) receptor in cardiomyocytes (Lee et al. 1993).

However, mechanical stress is by far the most important stimulus for the development of cardiac hypertrophy. Actually, mechanical stress induces a variety of hypertrophic responses in cardiomyocytes (Komuro and Yazaki 1993). Furthermore, pretreatment of cardiomyocytes with AT_1-receptor blockers (ARBs) significantly attenuates all of these mechanical stretch-induced hypertrophic responses (Sadoshima et al. 1993; Yamazaki et al. 1995). These results indicate that mechanical stress induces cardiac hypertrophy through the AT_1 receptor. It has been proposed

that AngII is stored in cardiomyocytes and that mechanical stretch induces the secretion of stored AngII into the culture medium, resulting in the induction of cardiomyocyte hypertrophy by the autocrine mechanism (Fig. 1a) (Sadoshima et al. 1993). However, we found a novel mechanism for mechanical stress-induced AT_1-receptor activation without the involvement of AngII, and discovered that this activation is inhibited by the inverse agonist candesartan (Fig. 1b) (Zou et al. 2004).

Mechanical stress-induced AT_1-receptor activation without the involvement of AngII

To examine whether AngII is secreted from cardiomyocytes into the culture medium by stretch, we first measured AngII concentration in the medium conditioned by stretching cardiomyocytes. We did not detect a significant increase in AngII concentration after stretch (AngII concentration without stretch, $0.7\pm1.6\times10^{-12}$ M; AngII concentration with stretch, $2.0\pm3.5\times10^{-12}$ M) (Zou et al. 2004). The concentration of AngII in the conditioned medium was not sufficient to evoke extracellular signal-regulated protein kinase (ERK) activation in cardiomyocytes, because the magnitude of ERK activation by stretch was equivalent to that observed when the cardiomyocytes were stimulated by 10^{-8} to 10^{-7} M of AngII (Zou et al. 2004). Furthermore, a neutralizing antibody to AngII did not suppress the stretch-induced ERK activation in cardiomyocytes, although the antibody abolished AngII (10^{-7} M)-induced ERK activation (Zou et al. 2004). These results suggest that stretch-induced ERK activation is largely dependent on AT_1 receptor, and that AngII, even if secreted from cardiomyocytes, plays a marginal role in stretch-induced ERK activation.

Next, to examine the possibility that mechanical stress can directly activate the AT_1 receptor without the involvement of AngII, we used human embryonic kidney (HEK) 293 cells and COS7 cells, neither of which showed a detectable expression of AT_1 receptor and angiotensinogen. Neither mechanical stretch nor AngII (10^{-7} M) activated ERKs in HEK293 cells (Fig. 2a), but forced expression of AT_1 receptor conferred the ability to activate ERKs in response to both mechanical stretch and AngII (Fig. 2b). Pretreatment with candesartan inhibited the ERK activation induced not only by AngII but also by mechanical stretch in HEK293 cells expressing AT_1 receptor (Fig. 2b). In addition, basal ERK activity was decreased by candesartan in HEK293 cells expressing AT_1 receptor (Fig. 2a,b) (Zou et al. 2004). Similar results were obtained in experiments using COS7 cells.

We also stretched HEK293 cells expressing AT_1-mutant receptor with impaired AngII binding (Yamano et al. 1992). AngII did not activate ERKs in these cells, as expected. However, ERKs were strongly activated by mechanical stretch, and this activation was inhibited by candesartan (Zou et al. 2004). To confirm whether mechanical stretch activates AT_1 receptor independently of AngII in cardiomyocytes, we stretched cardiomyocytes prepared from *angiotensinogen*-deficient mice, in which AngII is not produced (Tanimoto et al. 1994). Mechanical stretch activated ERKs in the cardiomyocytes prepared from both neonatal and adult *angiotensinogen*-deficient mice. Pretreatment with candesartan markedly suppressed stretch-induced ERK activation in these cells (Zou et al. 2004).

Finally, we examined whether mechanical stress could induce cardiac hypertrophy in vivo through the AT_1 receptor in the absence of AngII. We imposed a pressure overload on the heart by constricting the transverse aorta of adult male *angiotensinogen*-deficient mice. Pressure overload induced cardiac hypertrophy even in *angiotensinogen*-deficient mice (Fig. 2c). Furthermore, although treatment with candesartan did not reduce blood pressure in the right carotid artery, the

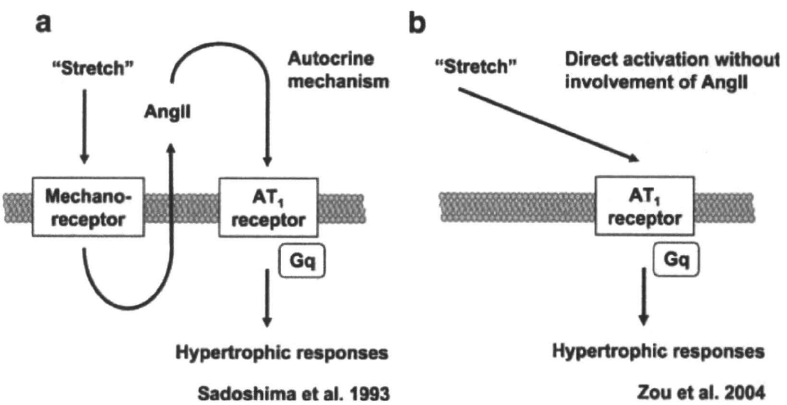

Fig. 1 A novel mechanism of mechanical stress-induced angiotensin II (AngII) type 1 (AT_1)-receptor activation without the involvement of AngII. **a** Mechanical stretch induces the secretion of stored AngII, and AngII subsequently evokes hypertrophic responses via AT_1 receptor by an autocrine mechanism (Sadoshima et al. 1993). **b** AT_1 receptor can be activated directly by mechanical stress through an AngII-independent mechanism (Zou et al. 2004)

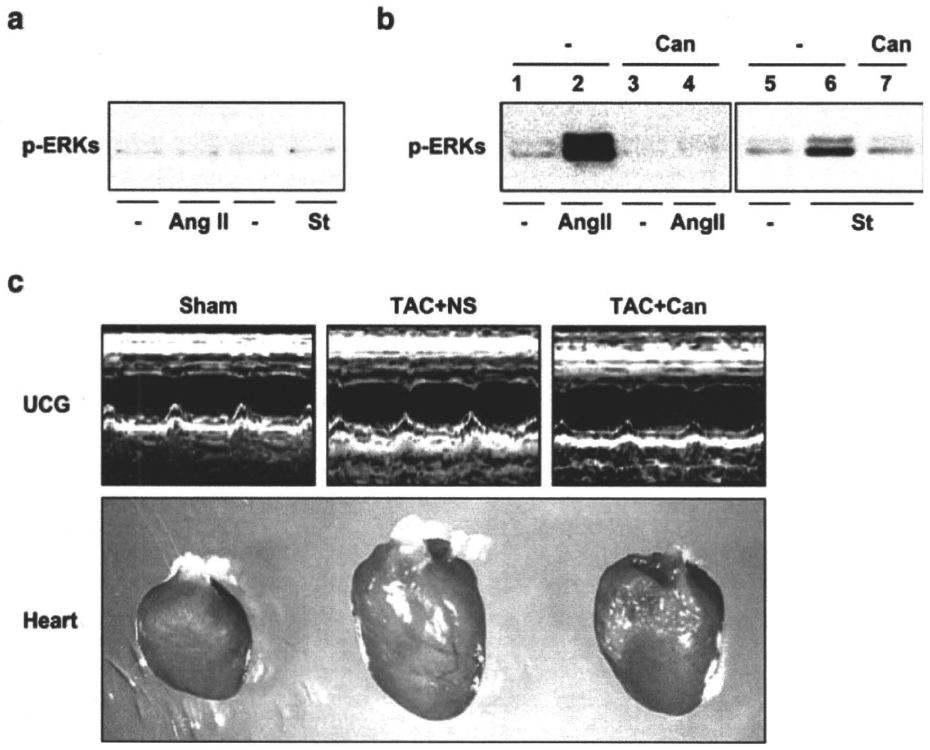

Fig. 2 Angiotensin II (AngII)-independent activation of ERKs via angiotensin II type 1 (AT_1) receptor by mechanical stretch. Modified from Zou et al. (2004). **a** Neither mechanical stretch nor AngII activated ERKs in HEK293 cells. HEK293 cells were stretched by 20% (*St*) or exposed to 10^{-7} M AngII for 8 min. **b** In HEK293 cells expressing AT_1 receptor, both mechanical stretch and AngII activated ERKs (*lanes 2* and *6*). Pretreatment with 10^{-7} M candesartan inhibited the activation of ERKs induced not only by AngII (*lane 4*) but also by mechanical stretch (*lane 7*). **c** Cardiac hypertrophy in *angiotensinogen*-deficient mice induced by pressure overload. Ten-week-old male *angiotensinogen*-deficient mice, treated with saline (*NS*) or candesartan (*Can*), were subjected to a sham or transverse aorta-constricting (*TAC*) operation. Echocardiography was done 2 weeks later. Pressure overload induced cardiac hypertrophy even in *angiotensinogen*-deficient mice. Pretreatment with candesartan attenuated this development. *Top* M-mode echocardiograms, *bottom* gross appearance of the heart

development of cardiac hypertrophy was significantly attenuated by candesartan (Fig. 2c) (Zou et al. 2004).

Based on these results, we proposed that mechanical stress activates the AT_1 receptor independently of AngII, which is inhibited by candesartan as an inverse agonist.

Mechanoreceptors and cardiac hypertrophy

Mechanical stress to cardiomyocytes is the most important stimulus that triggers hypertrophic responses (Komuro and Yazaki 1993), and we propose that the AT_1 receptor may be a receptor for mechanical stress. We previously reported that AT_1 receptor is not indispensable for load-induced cardiac hypertrophy, because pressure overload induced cardiac hypertrophy in AT_{1a}-receptor-knockout mice (Harada et al. 1998a, b). Interestingly, in *AT_{1a}-receptor*-deficient cardiomyocytes, basal activities of tyrosine kinase were upregulated and mechanical stretch induced stronger activation of tyrosine kinases than in wild-type cells, through epidermal growth factor (EGF)-receptor tyrosine kinases (Kudoh et al. 1998). These results suggest that some mechanisms compensate for the lack of AT_1 receptor and that pressure overload induces cardiac hypertrophy even in the absence of the AT_1 receptor.

AngII type 2 (AT_2) receptor is also a high-affinity receptor for AngII. We have not examined whether AT_2 receptor, like AT_1 receptor, is activated by mechanical stress because most of the known AngII functions in the cardiovascular system are mainly mediated through AT_1 receptor (Timmermans et al. 1993). Above all, the role of AT_2 receptor in cardiac hypertrophy remains enigmatic. In one study, aortic constriction caused cardiac hypertrophy to a similar degree in *AT_2-receptor*-deficient mice and wild-type mice (Wu et al. 2002). In contrast, in another study, cardiac hypertrophy was prevented after aortic constriction in *AT_2-receptor*-deficient mice compared with wild-type mice (Senbonmatsu et al. 2000).

Cardiac hypertrophy is induced by activation of other G-protein-coupled receptors (GPCRs) than AT_1 receptor, such as the receptors for endothelin 1 (ET-1) and catecholamines (Yamazaki et al. 1996; Zou et al. 1999). However, we found that mechanical stretch did not induce significant activation of ERKs in COS7 cells overexpressing either ET-1 type A

receptor or β2 adrenoceptor (Zou et al. 2004). Therefore, the activation of GPCRs by mechanical stretch without the involvement of their agonists is not a general phenomenon but specific to some GPCRs including AT_1 receptor.

At present, it remains unclear how the AT_1 receptor senses mechanical stress and translates it into biochemical signals inside the cells. There are a few hypothetical mechanisms by which mechanical stress could activate AT_1 receptor without the involvement of AngII. First, membrane tension may directly induce the conformational change in the AT_1 receptor. Second, mechanical stretch may activate specific mechanosensors, which subsequently activate the AT_1 receptor. Potential candidates for mechanosensors, such as muscle LIM protein within the Z-disc (Knoll et al. 2002), integrin-linked kinase (Bendig et al. 2006; White et al. 2006) and melusin (Brancaccio et al. 2003) within the costameres (band-like structures linking sarcolemmal membrane to Z-discs) and stretch-sensitive ion channels (Kung 2005; Orr et al. 2006), might activate the AT_1 receptor, although the underlying mechanism remains to be determined.

Inverse agonism of ARB

ARBs specifically inhibit the diverse physiological effects mediated by AT_1 receptor. ARBs not only have strong blood pressure-lowering effects in hypertensive patients, but also induce regression of left ventricular hypertrophy and decrease cardiovascular morbidity and mortality in patients with heart failure (Cohn and Tognoni 2001; Lindholm et al. 2002; Pfeffer et al. 2003). Many ARBs are available for clinical use, and they show unique pharmacological characters. The inverse-agonist activities of ARBs could be a novel and important pharmacological parameter defining the beneficial effects on organ protection.

Before the early 1990s, GPCR ligands were simply classified as agonists or antagonists (Bond and Ijzerman 2006). Both agonists and antagonists bind to GPCRs with high affinity; however, only agonists are able to activate the receptor. Therefore, agonists possess both high affinity and intrinsic activity, whereas antagonists possess high affinity without intrinsic activity. However, compounds that were originally described as antagonists were demonstrated to produce effects opposite to those observed with agonists (Costa and Herz 1989). Such ligands are classified as "inverse agonists." Inverse agonists, by definition, stabilize the inactive conformation of receptors and reduce the constitutive activity of the receptor or the agonist-independent receptor activity (Bond and Ijzerman 2006). In contrast, antagonists inhibit responses in competition with agonists, but they are not able to reduce the constitutive activity of the receptor or the agonist-independent receptor activity (Bond and Ijzerman 2006).

With regard to ARBs, it was reported that olmesartan and EXP3174 (active metabolite of losartan) reduce the constitutive activity of AT_1 mutant receptor (AT_1-N111G mutant), but losartan does not reduce them (Miura et al. 2003a; Miura et al. 2006). According to a recent paper, knockin mice with a constitutively activating mutation (AT_1-N111S with a C-terminal deletion) (AT_1-MUT mice) showed low-renin hypertension with relative hyperaldosteronism together with progressive renal and cardiac fibrosis (Billet et al. 2007). Interestingly, administration of candesartan, but not losartan, normalized blood pressure in AT_1-MUT mice. And, in mechanical stress-induced AT_1-receptor activation, candesartan inhibited mechanical stress-induced ERK activation (Zou et al. 2004), but losartan did not (unpublished data).

Some ARBs work as inverse agonists because they reduce the constitutive activity of AT_1 receptor or inhibit the agonist-independent mechanical-stress-induced AT_1-receptor activation. Recently, many clinical studies have shown that ARBs have excellent preventive effects on organ damage. ARBs with potent inverse-agonist activity may provide therapeutic benefits in the prevention of organ damage (Fig. 3).

Conformational change of GPCR

The AT_1 receptor, as well as other GPCRs, undergoes spontaneous isomerization among its inactive states (favored in the absence of agonist) and its active states (induced or stabilized by the agonist) (Gether 2000; Perez and Karnik 2005). In general, activation of GPCRs by agonists involves specific movements of the transmembrane (TM) helices following agonist binding (Gether 2000; Karnik et al. 2003).

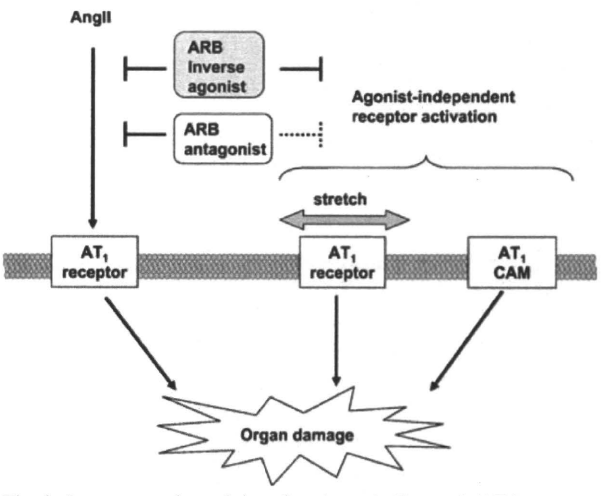

Fig. 3 Inverse-agonist activity of angiotensin II type 1 (AT_1)-receptor blockers (ARB). ARBs with potent inverse-agonist activities have therapeutic benefits in the prevention of organ damage because inverse agonists can inhibit agonist-independent-receptor activation by mechanical stress. *CAM* Constitutively active mutant

Structure–function analyses have demonstrated that the separation of TM3 and TM6 is a common structural change in GPCR activation (Gether 2000; Karnik et al. 2003). Agonist-induced activation of the β2 adrenoceptor involves disruption of an ionic lock between TM3 and TM6 (Yao et al. 2006). With regard to AT_1 receptor, the bindings of AngII to Asn^{111} in TM3 and to His^{256} in TM6 are crucial for receptor activation (Miura et al. 1999), and the mutations in Asn^{111} confer constitutive activity of the receptor (Feng et al. 1998; Groblewski et al. 1997) by releasing helical constraints involving TM2 (Miura and Karnik 2002; Miura et al. 2003b), TM6 (Martin et al. 2007) and TM7 (Boucard et al. 2003; Miura et al. 2003b).

Binding of an inverse agonist causes a transition of GPCR from a native, or partially active, state to an inactive state (Gether 2000; Perez and Karnik 2005) (Fig. 4). A recent study using a fluorescence resonance energy transfer (FRET) approach demonstrated that, in α_{2A}-adrenergic receptor, the conformational changes induced by an inverse agonist are different from those induced by an agonist (Vilardaga et al. 2005).

Our finding of mechanical stress-induced AT_1-receptor activation still leaves many issues to be solved, especially regarding mechanical stress-induced conformational change of AT_1 receptor. It would be a great challenge to determine the structural basis of how mechanical stress activates the AT_1 receptor and how candesartan exerts an inverse agonism.

Conclusions

We demonstrated that mechanical stress can induce cardiomyocyte hypertrophy both in vitro and in vivo through the AT_1 receptor without the involvement of AngII, and that these hypertrophic responses can be inhibited by candesartan, an ARB with potent inverse-agonist activity. A growing body of evidence has suggested that the local renin-angiotensin system plays an important role in injury to various organs (Bader et al. 2001; Baker et al. 1992; Lee et al. 1993). It remains to be determined whether activation of the AT_1 receptor without AngII occurs in other organs, and whether inverse agonists prevent organ damage more effectively than competitive antagonists. Further studies will be required to elucidate the exact molecular mechanisms of mechanical stress-induced AT_1-receptor activation and to clarify the clinical relevance of inverse-agonist activity of ARBs.

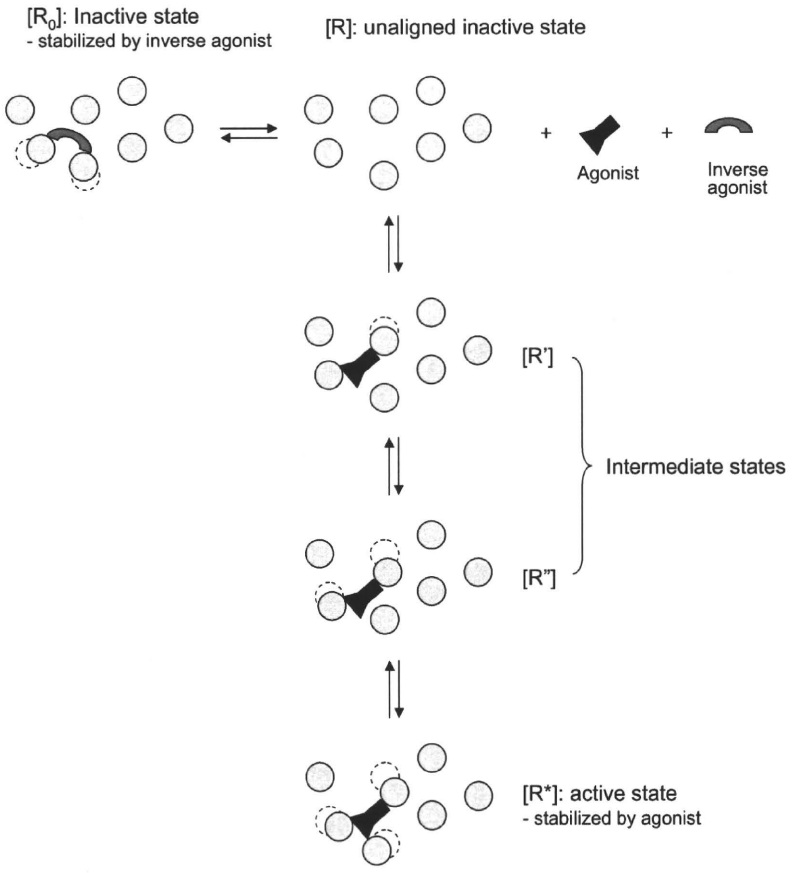

Fig. 4 Sequential binding and conformational stabilization model for the molecular mechanism of ligand action on G-protein-coupled receptors (GPCRs). Modified from Gether (2000). The hypothetical GPCR is represented by seven helices in gray, viewed from the extracellular side. The unaligned receptor exists in a unique state, [R], that can undergo transitions to at least two other stabilized states, $[R_0]$ and [R*]. $[R_0]$ is an inactive state stabilized by an inverse agonist, and [R*] is an active state stabilized by an agonist. Receptor activation occurs sequentially through a series of conformational changes. [R′] and [R″] are intermediate (partially active) states between [R] and [R*]

References

Bader M, Peters J, Baltatu O, Muller DN, Luft FC, Ganten D (2001) Tissue renin-angiotensin systems: new insights from experimental animal models in hypertension research. J Mol Med 79:76–102

Baker KM, Booz GW, Dostal DE (1992) Cardiac actions of angiotensin II: role of an intracardiac renin-angiotensin system. Annu Rev Physiol 54:227–241

Bendig G, Grimmler M, Huttner IG, Wessels G, Dahme T, Just S, Trano N, Katus HA, Fishman MC, Rottbauer W (2006) Integrin-linked kinase, a novel component of the cardiac mechanical stretch sensor, controls contractility in the zebrafish heart. Genes Dev 20:2361–2372

Billet S, Bardin S, Verp S, Baudrie V, Michaud A, Conchon S, Muffat-Joly M, Escoubet B, Souil E, Hamard G, Bernstein KE, Gasc JM, Elghozi JL, Corvol P, Clauser E (2007) Gain-of-function mutant of angiotensin II receptor, type 1A, causes hypertension and cardiovascular fibrosis in mice. J Clin Invest 117:1914–1925

Bond RA, Ijzerman AP (2006) Recent developments in constitutive receptor activity and inverse agonism, and their potential for GPCR drug discovery. Trends Pharmacol Sci 27:92–96

Boucard AA, Roy M, Beaulieu ME, Lavigne P, Escher E, Guillemette G, Leduc R (2003) Constitutive activation of the angiotensin II type 1 receptor alters the spatial proximity of transmembrane 7 to the ligand-binding pocket. J Biol Chem 278:36628–36636

Brancaccio M, Fratta L, Notte A, Hirsch E, Poulet R, Guazzone S, De Acetis M, Vecchione C, Marino G, Altruda F, Silengo L, Tarone G, Lembo G (2003) Melusin, a muscle-specific integrin beta1-interacting protein, is required to prevent cardiac failure in response to chronic pressure overload. Nat Med 9:68–75

Cohn JN, Tognoni G (2001) A randomized trial of the angiotensin-receptor blocker valsartan in chronic heart failure. N Engl J Med 345:1667–1675

Costa T, Herz A (1989) Antagonists with negative intrinsic activity at delta opioid receptors coupled to GTP-binding proteins. Proc Natl Acad Sci USA 86:7321–7325

Feng YH, Miura S, Husain A, Karnik SS (1998) Mechanism of constitutive activation of the AT1 receptor: influence of the size of the agonist switch binding residue Asn(111). Biochemistry 37:15791–15798

Gether U (2000) Uncovering molecular mechanisms involved in activation of G protein-coupled receptors. Endocr Rev 21:90–113

Groblewski T, Maigret B, Larguier R, Lombard C, Bonnafous JC, Marie J (1997) Mutation of Asn111 in the third transmembrane domain of the AT1A angiotensin II receptor induces its constitutive activation. J Biol Chem 272:1822–1826

Harada K, Komuro I, Shiojima I, Hayashi D, Kudoh S, Mizuno T, Kijima K, Matsubara H, Sugaya T, Murakami K, Yazaki Y (1998a) Pressure overload induces cardiac hypertrophy in angiotensin II type 1A receptor knockout mice. Circulation 97:1952–1959

Harada K, Komuro I, Zou Y, Kudoh S, Kijima K, Matsubara H, Sugaya T, Murakami K, Yazaki Y (1998b) Acute pressure overload could induce hypertrophic responses in the heart of angiotensin II type 1a knockout mice. Circ Res 82:779–785

Karnik SS, Gogonea C, Patil S, Saad Y, Takezako T (2003) Activation of G-protein-coupled receptors: a common molecular mechanism. Trends Endocrinol Metab 14:431–437

Knoll R, Hoshijima M, Hoffman HM, Person V, Lorenzen-Schmidt I, Bang ML, Hayashi T, Shiga N, Yasukawa H, Schaper W, McKenna W, Yokoyama M, Schork NJ, Omens JH, McCulloch AD, Kimura A, Gregorio CC, Poller W, Schaper J, Schultheiss HP, Chien KR (2002) The cardiac mechanical stretch sensor machinery involves a Z disc complex that is defective in a subset of human dilated cardiomyopathy. Cell 111:943–955

Komuro I, Yazaki Y (1993) Control of cardiac gene expression by mechanical stress. Annu Rev Physiol 55:55–75

Kudoh S, Komuro I, Hiroi Y, Zou Y, Harada K, Sugaya T, Takekoshi N, Murakami K, Kadowaki T, Yazaki Y (1998) Mechanical stretch induces hypertrophic responses in cardiac myocytes of angiotensin II type 1a receptor knockout mice. J Biol Chem 273:24037–24043

Kung C (2005) A possible unifying principle for mechanosensation. Nature 436:647–654

Lee MA, Bohm M, Paul M, Ganten D (1993) Tissue renin-angiotensin systems. Their role in cardiovascular disease. Circulation 87: IV7–13

Levy D, Garrison RJ, Savage DD, Kannel WB, Castelli WP (1990) Prognostic implications of echocardiographically determined left ventricular mass in the Framingham Heart Study. N Engl J Med 322:1561–1566

Lindholm LH, Ibsen H, Dahlof B, Devereux RB, Beevers G, de Faire U, Fyhrquist F, Julius S, Kjeldsen SE, Kristiansson K, Lederballe-Pedersen O, Nieminen MS, Omvik P, Oparil S, Wedel H, Aurup P, Edelman J, Snapinn S (2002) Cardiovascular morbidity and mortality in patients with diabetes in the Losartan Intervention For Endpoint reduction in hypertension study (LIFE): a randomised trial against atenolol. Lancet 359:1004–1010

Martin SS, Holleran BJ, Escher E, Guillemette G, Leduc R (2007) Activation of the angiotensin II type 1 receptor leads to movement of the sixth transmembrane domain: analysis by the substituted cysteine accessibility method. Mol Pharmacol 72:182–190

Miura S, Karnik SS (2002) Constitutive activation of angiotensin II type 1 receptor alters the orientation of transmembrane helix-2. J Biol Chem 277:24299–24305

Miura S, Feng YH, Husain A, Karnik SS (1999) Role of aromaticity of agonist switches of angiotensin II in the activation of the AT1 receptor. J Biol Chem 274:7103–7110

Miura S, Saku K, Karnik SS (2003a) Molecular analysis of the structure and function of the angiotensin II type 1 receptor. Hypertens Res 26:937–943

Miura S, Zhang J, Boros J, Karnik SS (2003b) TM2-TM7 interaction in coupling movement of transmembrane helices to activation of the angiotensin II type-1 receptor. J Biol Chem 278:3720–3725

Miura S, Fujino M, Hanzawa H, Kiya Y, Imaizumi S, Matsuo Y, Tomita S, Uehara Y, Karnik SS, Yanagisawa H, Koike H, Komuro I, Saku K (2006) Molecular mechanism underlying inverse agonist of angiotensin II type 1 receptor. J Biol Chem 281:19288–19295

Orr AW, Helmke BP, Blackman BR, Schwartz MA (2006) Mechanisms of mechanotransduction. Dev Cell 10:11–20

Perez DM, Karnik SS (2005) Multiple signaling states of G-protein-coupled receptors. Pharmacol Rev 57:147–161

Pfeffer MA, Swedberg K, Granger CB, Held P, McMurray JJ, Michelson EL, Olofsson B, Ostergren J, Yusuf S, Pocock S (2003) Effects of candesartan on mortality and morbidity in patients with chronic heart failure: the CHARM-Overall programme. Lancet 362:759–766

Sadoshima J, Xu Y, Slayter HS, Izumo S (1993) Autocrine release of angiotensin II mediates stretch-induced hypertrophy of cardiac myocytes in vitro. Cell 75:977–984

Senbonmatsu T, Ichihara S, Price Jr E, Gaffney FA, Inagami T (2000) Evidence for angiotensin II type 2 receptor-mediated cardiac myocyte enlargement during in vivo pressure overload. J Clin Invest 106:R25–29

Tanimoto K, Sugiyama F, Goto Y, Ishida J, Takimoto E, Yagami K, Fukamizu A, Murakami K (1994) Angiotensinogen-deficient mice with hypotension. J Biol Chem 269:31334–31337

Timmermans PB, Wong PC, Chiu AT, Herblin WF, Benfield P, Carini DJ, Lee RJ, Wexler RR, Saye JA, Smith RD (1993) Angiotensin

II receptors and angiotensin II receptor antagonists. Pharmacol Rev 45:205–251

Vilardaga JP, Steinmeyer R, Harms GS, Lohse MJ (2005) Molecular basis of inverse agonism in a G protein-coupled receptor. Nat Chem Biol 1:25–28

White DE, Coutu P, Shi YF, Tardif JC, Nattel S, St Arnaud R, Dedhar S, Muller WJ (2006) Targeted ablation of ILK from the murine heart results in dilated cardiomyopathy and spontaneous heart failure. Genes Dev 20:2355–2360

Wu L, Iwai M, Nakagami H, Chen R, Suzuki J, Akishita M, de Gasparo M, Horiuchi M (2002) Effect of angiotensin II type 1 receptor blockade on cardiac remodeling in angiotensin II type 2 receptor null mice. Arterioscler Thromb Vasc Biol 22:49–54

Yamano Y, Ohyama K, Chaki S, Guo DF, Inagami T (1992) Identification of amino acid residues of rat angiotensin II receptor for ligand binding by site directed mutagenesis. Biochem Biophys Res Commun 187:1426–1431

Yamazaki T, Komuro I, Kudoh S, Zou Y, Shiojima I, Mizuno T, Takano H, Hiroi Y, Ueki K, Tobe K (1995) Angiotensin II partly mediates mechanical stress-induced cardiac hypertrophy. Circ Res 77:258–265

Yamazaki T, Komuro I, Kudoh S, Zou Y, Shiojima I, Hiroi Y, Mizuno T, Maemura K, Kurihara H, Aikawa R, Takano H, Yazaki Y (1996) Endothelin-1 is involved in mechanical stress-induced cardiomyocyte hypertrophy. J Biol Chem 271:3221–3228

Yao X, Parnot C, Deupi X, Ratnala VR, Swaminath G, Farrens D, Kobilka B (2006) Coupling ligand structure to specific conformational switches in the beta2-adrenoceptor. Nat Chem Biol 2:417–422

Zou Y, Komuro I, Yamazaki T, Kudoh S, Uozumi H, Kadowaki T, Yazaki Y (1999) Both Gs and Gi proteins are critically involved in isoproterenol-induced cardiomyocyte hypertrophy. J Biol Chem 274:9760–9770

Zou Y, Akazawa H, Qin Y, Sano M, Takano H, Minamino T, Makita N, Iwanaga K, Zhu W, Kudoh S, Toko H, Tamura K, Kihara M, Nagai T, Fukamizu A, Umemura S, Iiri T, Fujita T, Komuro I (2004) Mechanical stress activates angiotensin II type 1 receptor without the involvement of angiotensin II. Nat Cell Biol 6:499–506

Deficiency of *Myo18B* in mice results in embryonic lethality with cardiac myofibrillar aberrations

Rieko Ajima[1,a], Hiroshi Akazawa[2], Maho Kodama[3], Fumitaka Takeshita[3], Ayaka Otsuka[1], Takashi Kohno[1], Issei Komuro[2], Takahiro Ochiya[3] and Jun Yokota[1,*]

[1]*Biology Division and* [3]*Section for Studies on Metastasis, National Cancer Center Research Institute, Tokyo 104-0045, Japan*
[2]*Department of Cardiovascular Science and Medicine, Chiba University Graduate School of Medicine, Chiba 260-8677, Japan*

Myo18B is an unconventional myosin family protein expressed predominantly in muscle cells. Although conventional myosins are known to be localized on the A-bands and function as a molecular motor for muscle contraction, Myo18B protein was localized on the Z-lines of myofibrils in striated muscles. Like Myo18A, another 18th class of myosin, the N-terminal unique domain of the protein and not the motor domain and the coiled-coil tail is critical for its localization to F-actin in myocytes. Myo18B expression was induced by myogenic differentiation through the binding of myocyte-specific enhancer factor-2 to its promoter. Deficiency of Myo18B caused an embryonic lethality in mice accompanied by disruption of myofibrillar structures in cardiac myocytes at embryonic day 10.5. Thus, Myo18B is a unique unconventional myosin that is predominantly expressed in myocytes and whose expression is essential for the development and/or maintenance of myofibrillar structure.

Introduction

Myosins constitute a large superfamily of actin-based motor proteins that use ATP to play fundamental roles in many forms of eukaryotic cell motility, such as cell migration, cytokinesis, phagocytosis, and trafficking. A total of 40 myosin genes have been identified in humans to date; however, physiological and biological functions of more than half of their products are still unknown. (Mermall *et al.* 1998; Wu *et al.* 2000; Berg *et al.* 2001). We previously isolated a novel unconventional myosin, MYO18B, from a homozygously deleted region at chromosome 22q12.1 in a human lung cancer cell line (Nishioka *et al.* 2002). Inactivation of this gene by genetic and/or epigenetic alterations in human cancer cells suggests that the *MYO18B* gene functions as a tumor suppressor in human carcinogenesis (Nishioka *et al.* 2002; Tani *et al.* 2004; Yanaihara *et al.* 2004; Nakano *et al.* 2005). Like other myosins, MYO18B has a myosin head motor domain with an ATP-binding motif and a GPA actin-binding motif. It also contains a neck region with an IQ motif that is thought to participate in binding to myosin light chains or calmodulin and a C-terminal tail with a coiled-coil domain that likely mediates dimer formation. Furthermore, MYO18B has unique N- and C-terminal extensions (Fig. 1A), which should give a distinction against other classes of myosins. However, physiological functions of MYO18B are largely unknown. Here, we showed the N-terminal unique domain of MYO18B is crucial for its localization to F-actin, and analysis of *Myo18B* gene targeted mice revealed that Myo18B protein is crucial for the development and/or maintenance of myofibrillar structure in myocytes.

Communicated by: Fuyuki Ishikawa
**Correspondence*: jyokota@gan2.ncc.go.jp
[a]*Current address*: Cell and Developmental Biology Laboratory, National Cancer Institute-Frederick, NIH, MD 21702, USA.

Results

Contribution of N-terminal extension of Myo18B protein to its localization on F-actin

To characterize the functions of Myo18B, we used C2C12 cells because the *Myo18B* transcription is increased by myogenic differentiation in C2C12 mouse myoblast cells (Salamon *et al.* 2003). Western blot analysis reveals that endogenous Myo18B protein level increases along with C2C12 cells differentiation (Fig. 1B). Then, we carried out immunofluorescence analysis of C2C12 cells using two independent antibodies against Myo18B. Endogenous Myo18B protein stained very faintly in undifferentiated C2C12 cells, but better in multinucleated differentiated

DOI: 10.1111/j.1365-2443.2008.01226.x

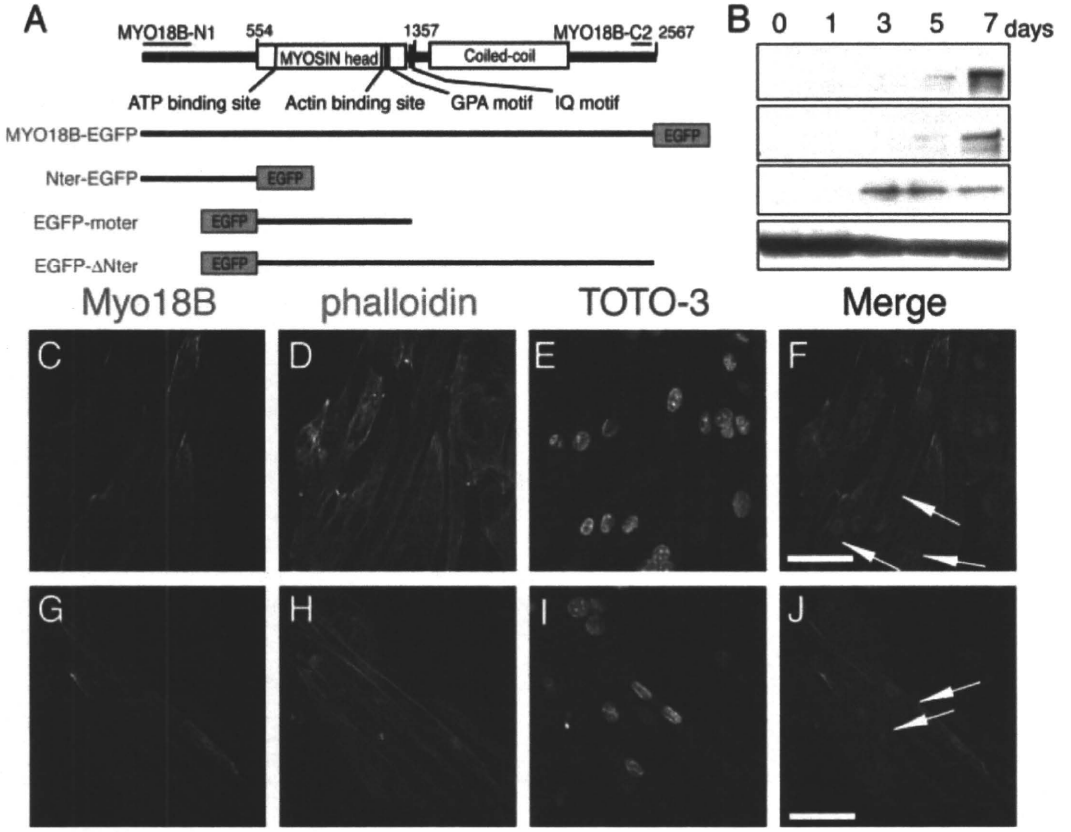

Figure 1 Intracellular localization of endogenous and deletion mutants of Myo18B protein in C2C12 cells. (A) Structure of MYO18B protein, positions of antigens for antibodies and EGFP-fusion protein structures used below are shown. (B) Western blot analysis of C2C12 cells with induction of myogenic differentiation using antibodies, anti-MYO18B-N1 (upper panel), anti-MYO18B-C2 (upper middle panel), anti-Myogenin (lower middle panel), and anti-α tubulin (lower panel). Confocal images of immunocytochemistry of differentiated C2C12 cells (C–J) using anti-MYO18B-N1 (C and green in F) and anti-MYO18B-C2 (G and green in J) are shown. Arrows in F and J indicate differentiated and multinucleated C2C12 cells. Localization of EGFP-fusion deletion mutants of MYO18B is shown (K–Z). MYO18B-EGFP (K–N), Nter-EGFP (O–R), EGFP-moter (S–V) and EGFP-ΔNter (W–Z) were expressed in C2C12 cells. The cells were co-stained with phalloidin (D, H, L, P, T, X and red in F, J, N, R, V, Z) and TOTO-3 (E, I, M, Q, U, Y and blue in F, J, N, R, V, Z). Bars = 50 μm (F), 20 μm (J, N, R, V, Z).

C2C12 cells that were positive for myoglobin and skeletal myosin (data not shown). This result is consistent with the result of Western blot analysis. In differentiated C2C12 cells, Myo18B was predominantly distributed on F-actin with a punctate pattern (Fig. 1C–J). Previously Myo18B protein was reported to be localized in the nucleus of differentiated C2C12 cells and striated muscles (Salamon *et al.* 2003); however, the antibodies did not indicate a nuclear distribution of Myo18B protein in both differentiated C2C12 cells and striated muscles.

To reveal which domain of Myo18B contributes to the localization on F-actin, we prepared expression vectors for EGFP-fused MYO18B full-length (MYO18B-EGFP) protein and for deletion mutants (Fig. 1A). Exogenously expressed MYO18B-EGFP in C2C12 cells was predominantly distributed on actin stress fibers as endogenous Myo18B, and localized in cytoplasm with a punctate pattern (Fig. 1K–N). When cells had a protruded region, which is a region where F-actin is actively polymerized, MYO18B-EGFP co-localized to these sites as well (data not shown) consistent with results shown previously in NIH3T3 cells (Ajima *et al.* 2007). Analysis of an EGFP-fused N-terminal half (1–1357 a.a.) and C-terminal half (1357–2567 a.a.) of MYO18B protein revealed that the N-terminal half of MYO18B is necessary, but dimerization with a coiled-coil domain in the C-terminal half of MYO18B, is not necessary for localization on F-actin (data not shown). The N-terminal half of MYO18B was

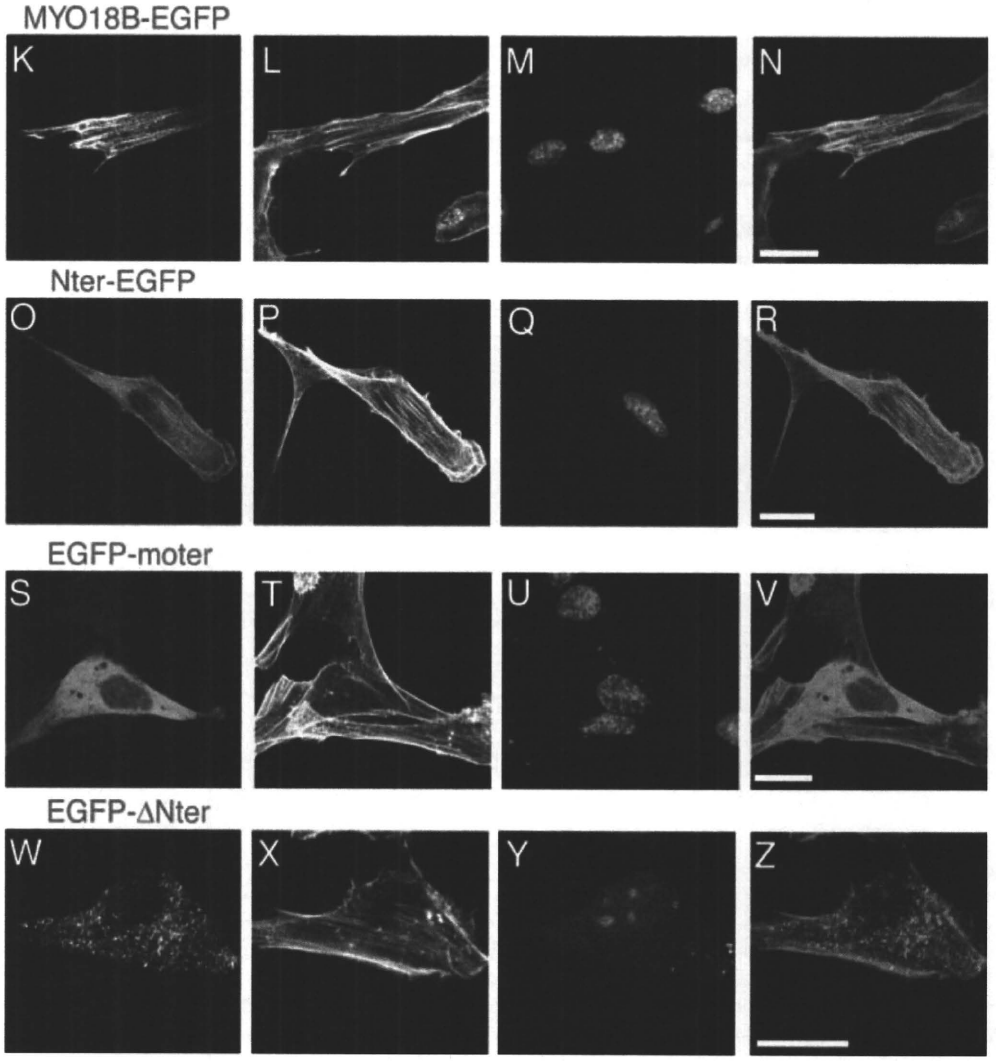

Figure 1 *Continued*

further divided into the N-terminal extension (Nter-EGFP) and the motor region (EGFP-moter) and both were expressed in C2C12 cells. EGFP-moter was homogenously distributed throughout the cytoplasm (Fig. 1S–V), whereas Nter-EGFP was localized clearly on F-actin (Fig. 1O–R). A vector of MYO18B without the N-terminal extension (EGFP-ΔNter) was also expressed. EGFP-ΔNter was localized in the cytoplasm with a punctate pattern as MYO18B-EGFP, but its localization on actin stress fibers was unclear (Fig. 1W–Z). Taking these results together, it was concluded that the N-terminal extension of MYO18B protein greatly contributes to the localization of MYO18B on actin stress fibers.

Intracellular localization of Myo18B protein in striated muscle cells

To reveal the localization of Myo18B protein in skeletal and cardiac muscles, we carried out immunohistochemistry using anti-MYO18B antibodies. Myo18B showed a stripe pattern in muscle cells, suggesting that Myo18B is localized in either the A-bands or the Z-lines. The cells were co-stained with an α-actinin antibody, a marker of the Z-lines. α-actinin showed a stripe pattern in the same region, but the bands for α-actinin were thinner and sharper than those for Myo18B. The result indicated that Myo18B is localized in the Z-lines and in the

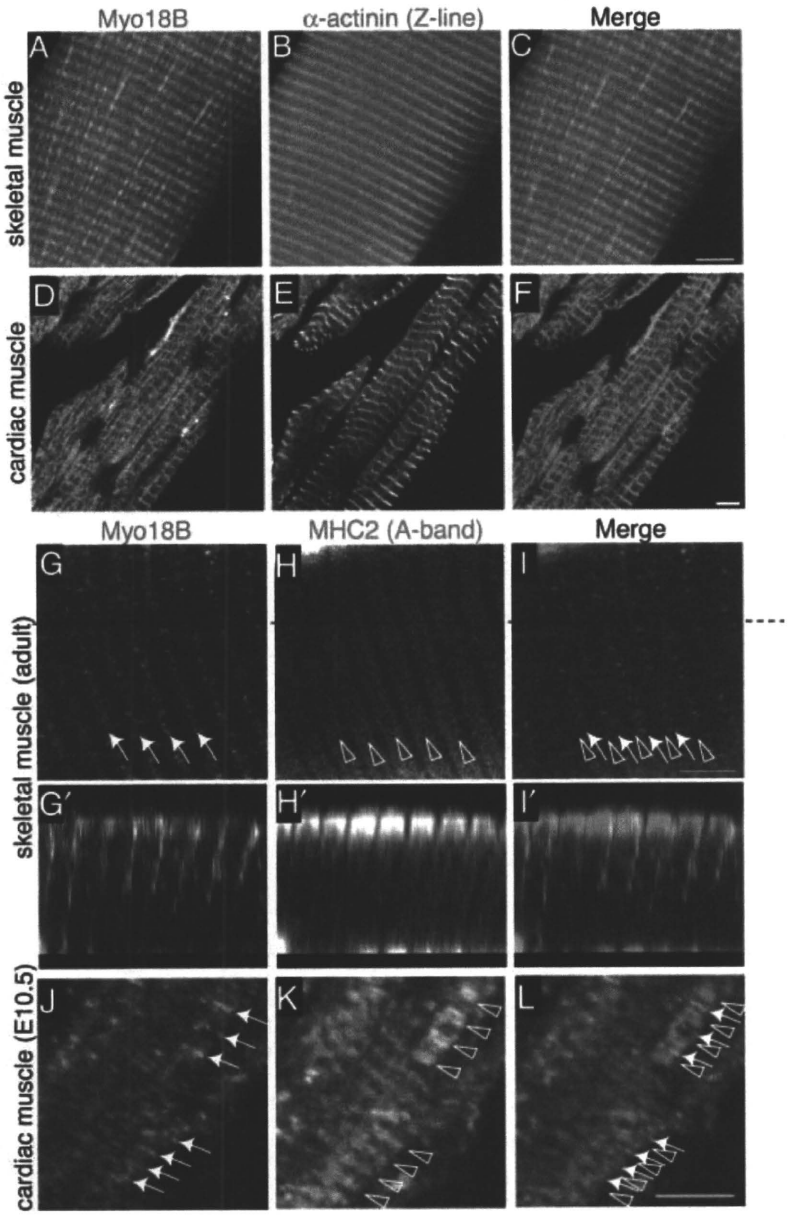

Figure 2 Intracellular localization of endogenous Myo18B protein in striated muscles. Confocal images of frozen sections of skeletal muscle (A, B, C and G, G′, H, H′, I, I′), cardiac muscle (D, E, F) of adult mice and sections of paraffin embedded cardiac muscle of an E10.5 embryo (J, K, L) that are immunohistochemically stained with anti-MYO18B-N1 (A, D, G, G′, J and green in C, F, I, I′, L), anti-α-actinin (B, E and red in C, F), anti-skeletal myosin (H, H′ and red in I, I′) and anti-myosin heavy chain β (K and red in L) antibodies are shown. The localization of Myo18B is indicated by arrows and that of the A-bands is indicated by triangles (G–L). X–Z scan at the doted line in G, H, I, along the longitudinal axes of myocytes are shown in G′, H′, I′. Bars = 5 μm.

region adjacent to the Z-lines in both skeletal and cardiac muscles (Fig. 2A,B,C and D,E,F). Co-staining of Myo18B with type II myosin showed that Myo18B did not co-localize with type II myosin in adult skeletal muscles (Fig. 2G,G′,H,H′,I,I′) or in cardiac muscles of E10.5 wild-type embryos, either (Fig. 2J,K,L). A confocal X-Z scan image confirmed that Myo18B was localized in myofibrils between the A-bands (Fig. 2G′,H′,I′). These results suggest that Myo18B is not used as a molecular motor in the A-bands for muscle contraction and plays a distinct role from conventional myosins.

Regulation of Myo18B expression in myogenic differentiation of C2C12 mouse myoblast cells

Because Myo18B protein is induced by myogenic differentiation, Myo18B gene expression could be strictly regulated by myogenic transcriptional factors. To analyze the transcriptional regulation of the *Myo18B* gene, we

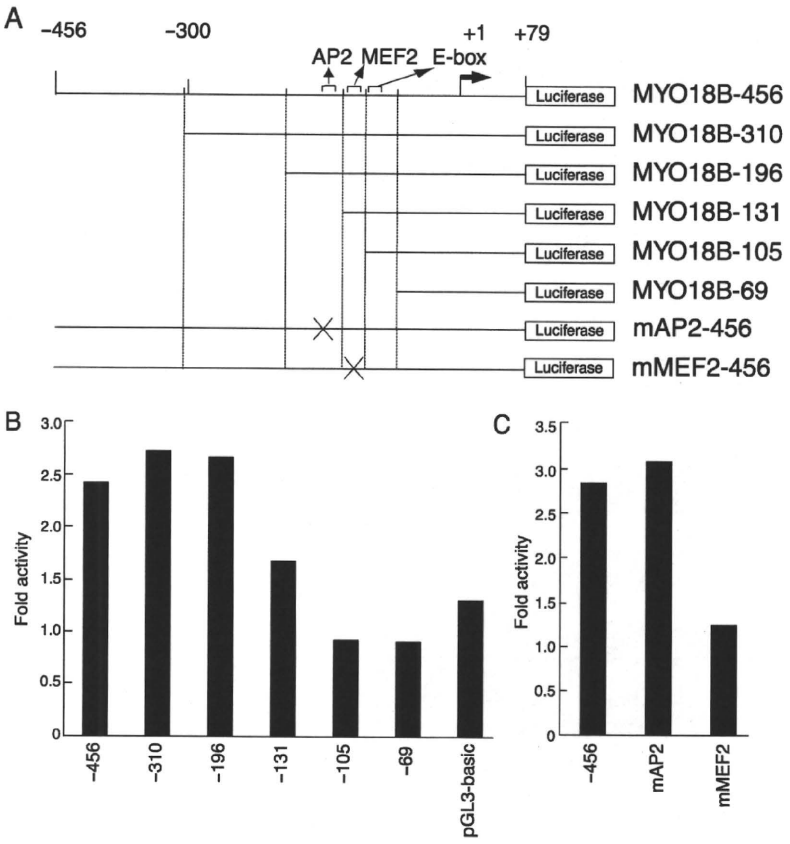

Figure 3 Regulation of Myo18B expression during differentiation of C2C12 myoblasts. (A) Schematic representation of the *MYO18B* gene promoter region and deletion constructs. The positions of transcriptional factor-response elements that are conserved in humans and mice and the position of the transcriptional start site (+1) are shown above a wild type *MYO18B* promoter construct, MYO18B-456. (B and C) Fold luciferase activities of several *MYO18B* promoter constructs compare with undifferentiated and differentiated C2C12 cells. The luciferase activities of MYO18B-456, six promoter deletion constructs (–310, –196, –131, –105, and –69 in B), and mutant constructs for AP2 and MEF2 responsible elements (mAP2 and mMEF2, respectively in C) in C2C12 cells were determined by transfecting the cells with each construct. Fold activities were calculated by dividing differentiated C2C12 cells activity with undifferentiated C2C12 cells activity. Constructs were used more than 3 times and showed similar results.

compared the genomic structure in the 5′ region of the human *MYO18B* and mouse *Myo18B* genes using the ClustalW multiple sequence alignment program (http://align.genome.jp/). The nucleotide sequence between the –350 nucleotide and a putative transcription start site (+1) of the human gene was highly conserved in the mouse gene. Furthermore, we screened repetitive elements upstream of the promoter region of the *Myo18B* gene using the RepeatMasker program (http://www.repeatmasker.org). Repetitive elements started roughly 500 nucleotides upstream from the putative transcription start site (Fig. 3A). Therefore, to define the critical elements for regulation of Myo18B mRNA expression in myocytes and during their differentiation, a series of *MYO18B* promoter deletion constructs were cloned with reporter vectors for the luciferase assay (Fig. 3A). These vectors were introduced into C2C12 cells and the differentiation was induced. The MYO18B-456 promoter activity in differentiated C2C12 cells was 2–3 times higher than that in undifferentiated cells. The induction of promoter activity was kept with MYO18B-310 and MYO18B-196 constructs, but was decreased with the MYO18B-131 construct and diminished with MYO18B-105 or –69 constructs (Fig. 3B). So, the segments of nucleotides –196 to –131 and –131 to –105 of the *MYO18B* gene were suggested to bear an enhancer element for myocyte differentiation. A putative AP2-response element was present between nucleotides –196 and –131, and an AT-rich putative MEF2-response element was between nucleotides –131 and –105, and both element were conserved in human and mouse (Fig. 3A). Therefore, reporter vectors with a mutation in each putative binding site of the *MYO18B* promoter were further constructed. A reporter construct with a mutation in the putative AP2-response element showed similar promoter activity as MYO18B-456 promoter. In contrast, a reporter construct with a mutation in the putative MEF2-response element showed slight induction by myogenic differentiation (Fig. 3C). These results suggest that MEF2 plays an important role in the induction of Myo18B expression in myocytes.

Generation of Myo18B gene targeting mice and embryonic lethality of homozygous knockouts

A targeting vector was constructed by insertion of the bacterial *nls-LacZ* and *NeoR* genes into exon 2 containing

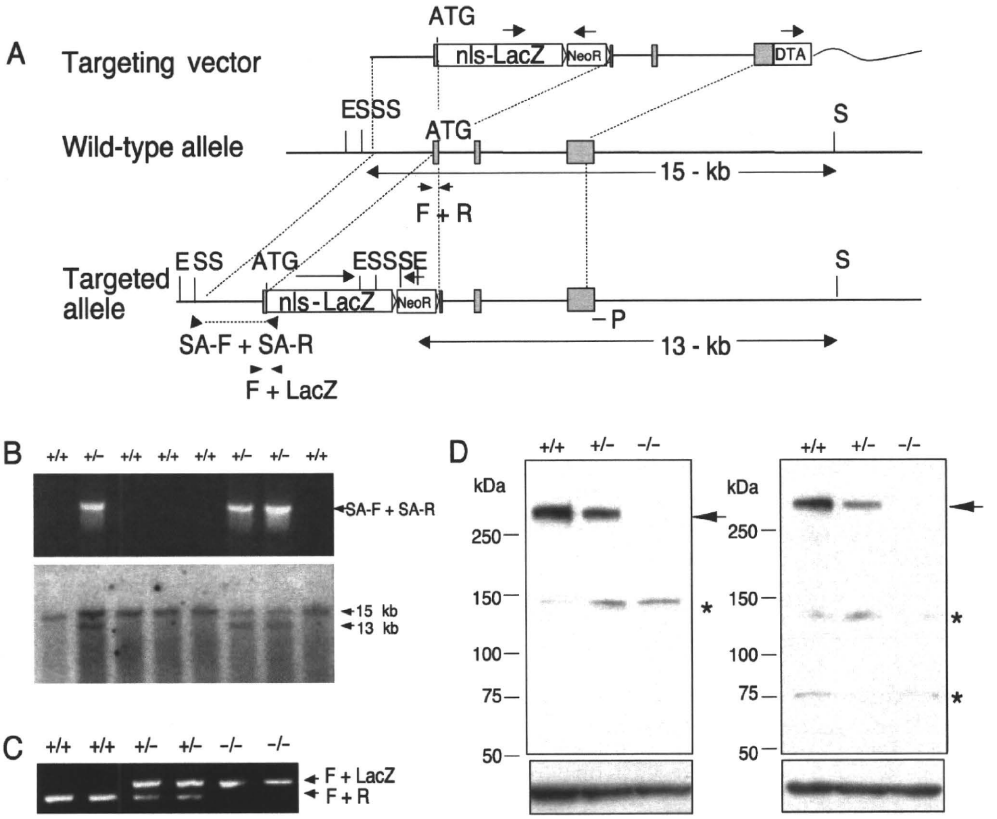

Figure 4 Targeted disruption of the mouse *Myo18B* gene and its expression. (A) Targeting strategy with the targeting vector (*top*), a restriction map of the wild-type *Myo18B* allele covering exon 2 to exon 4 (*middle*), and the targeted allele disrupted by a homologous recombination (*bottom*) are shown. ATG, SA-F + SA-R; PCR primer sets for ES screening and genotyping for short arm, F + R; PCR primer sets for genotyping wild-type allele, and F + LacZ; PCR primer sets for genotyping targeted allele, P; probe for Southern blot analysis, and 15-kb/13-kb of the expected fragment lengths are indicated. E, *EcoRI*; S, *SphI*; *nls-LacZ*; nuclear localization signal-*β-galactosidase* gene, *NeoR*; neomycin resistant gene, *DTA*; *Diphtheria toxin A* gene. Arrows above gene cassettes indicate the direction of the genes. (B) Representative results of PCR and Southern blot analyses for genotyping of ES cells and F1 mice are shown. The 2.2-kb PCR fragments represent a disrupted allele (upper), and 15 kb and 13 kb *EcoRI/SphI* genomic DNA fragments represent the wild-type and the disrupted alleles, respectively (lower). (C) Representative results of PCR-mediated genotyping of embryos are shown. The primers are shown by arrows in A. +/+, *Myo18*$^{+/+}$; +/–, *Myo18*$^{+/-}$; and –/–, *Myo18*$^{-/-}$. (D) Results of Western blot analysis for Myo18B protein in cultured whole embryo are shown. Upper left and right panels are blots by anti-MYO18B-N1 and anti-MYO18B-C2 antibodies, respectively. Both lower panels are blots by anti α-tubulin antibody. Myo18B protein is indicated by arrows, and non-specific bands are indicated by*.

the translation initiation codon of the mouse *Myo18B* gene (Fig. 4A). Two independent *Myo18*$^{+/-}$ES cell clones, 109 and 153, were established, used to make *Myo18* mutant chimeric and heterozygous mice. Targeting disruption of the gene in ES clones and heterozygous mice was confirmed by PCR and Southern blot analyses (Fig. 4B). The mice appeared healthy and fertile, with no indication of physical abnormalities.

Heterozygous mice were then mated to obtain mice with Myo18B deficiency. However, no live *Myo18B*$^{-/-}$ offspring was born from either line, implying that *Myo18B*$^{-/-}$ embryos had died during embryogenesis. To determine the time of death, embryos from different developmental stages were genotyped by PCR (Fig. 4C) and macroscopically inspected (Table 1). Up to E10, the expected Mendelian ratio of viable *Myo18B*$^{-/-}$ embryos was observed. However, at E10.5 to E11, 12 of 31 *Myo18B*$^{-/-}$ embryos were abnormal and 4 empty deciduas were observed. At E11.5 to E13.5, none of the remaining 9 *Myo18B*$^{-/-}$ embryos were normal and the number of empty deciduas increased. *Myo18B*$^{-/-}$ dead embryos were shown to have either dilated pericardial cavities, internal hemorrhage or resorption.

Table 1 Genotypes and phenotypes of Myo18B heterozygous intercrosses

		Total	*Myo18B*$^{+/+}$	*Myo18B*$^{+/-}$	*Myo18B*$^{-/-}$ (D/V)*	Empty decidua	Aspects of *Myo18B*$^{-/-}$ dead embryos†
Newborn	line 153	112	50	62	0		
	line 109	107	40	67	0		
Embryo (line 153)	E11.5-13.5	55	14	24	9 (9/0)	8	1D; 1H; 7R
	E10.5-11	139	37	67	31 (12/19)	4	1D; 7H; 4R
	E9.5-10	74	13	37	19 (0/19)	0	

*The number of dead (D) and viable (V) embryos is shown as D/V in parentheses.
†The number of Myo18B dead embryos with dilated pericardiac cavity (D), internal hemorrhage (H), and resorption (R) is shown.

To verify the knockout of the targeted region, Western blot analysis with lysates of cultured whole embryos (Fig. 4D) were carried out. A prominent 290-kD band was detected in the lysate of wild-type (*Myo18B*$^{+/+}$) embryos. The intensity of the band decreased in *Myo18B*$^{+/-}$ embryos, and the band disappeared in *Myo18B*$^{-/-}$ embryos.

Myo18B expression probed by the knocked-in bacterial LacZ gene in *Myo18*$^{+/-}$ mice

β-Galactosidase, the gene product of *nls-LacZ*, generates blue signals by hydrolyzing X-Gal. Therefore, the knocked-in *nls-LacZ* gene under the transcriptional control of the endogenous *Myo18B* promoter signals the pattern of *Myo18B* mRNA expression in *Myo18*$^{+/-}$ embryos and mice. The whole mount X-Gal staining of *Myo18*$^{+/-}$ embryos revealed that *nls-LacZ* was expressed in heart and somites at E9.5 and E11.5 (Fig. 5A–C). At E13.5, *nls-LacZ* expression was prominent in muscles of the cardiac atriums and ventricles (Fig. 5D left and lower right panel), and was also detected in myotomes and muscle mass (Fig. 5D left and upper right panel). In *Myo18*$^{+/-}$ adult mice, *nls-LacZ* was expressed prominently in cardiac and skeletal muscles (Fig. 5E,F) as well as in smooth muscles of several tissues, and in some parts of testis and brain (data not shown). The pattern of Myo18B expression indicated by X-gal staining was similar to that previously shown by tissue Northern blot analysis (Salamon *et al.* 2003).

Cardiac defects in *Myo18B*$^{-/-}$ embryos

Macroscopically, the *Myo18B*$^{-/-}$ embryos appeared to be normal in early developmental stages, with no detectable abnormality up to E9.5. Abnormal embryos were found as early as E10.5. From E10.5 to E13.5, the number of resorbed or growth-retarded embryos (Fig. 6D) increased, and some unresorbed *Myo18B*$^{-/-}$ embryos showed severe internal hemorrhage in the cardiac and ventral body wall regions (Fig. 6B) or pericardiac cavity dilation (Fig. 6H).

Therefore, *Myo18B*$^{-/-}$ embryos and control (*Myo18B*$^{+/+}$ and *Myo18B*$^{+/-}$ embryos) littermates were histologically analyzed at various developmental stages. At E9.5, *Myo18B*$^{-/-}$ embryos showed a normal looping of the linear heart tube and correct cardiac morphology compared with control embryos (data not shown). At E10.5, the formation of the cardiac chambers was initiated correctly in *Myo18B*$^{-/-}$ embryos that were neither resorbed nor hemorrhagic. However, some *Myo18B*$^{-/-}$ embryos at E10.5 to E12.5 showed striking abnormalities in the myocardium (Fig. 6F,H). Variable degrees of pericardial effusion were observed (Fig. 6H). The lumens of both the right and left cardinal veins and the right atrium in *Myo18B*$^{-/-}$ embryos were morbidly enlarged (Fig. 6F,H) when compared with controls (Fig. 6E,G).

Abnormal myofibrillar organization in *Myo18B*$^{-/-}$ cardiac myocytes

Ultrastructural analysis of comparable areas from the left ventricular free walls of *Myo18B*$^{+/+}$ and *Myo18B*$^{-/-}$ embryos revealed abnormalities in sarcomeric assembly in the *Myo18B*$^{-/-}$ embryos. *Myo18B*$^{-/-}$ cardiac myocytes had normal sarcomeres length with structures of intercalated disks and Z-lines, but displayed a disorganized alignment of parallel thick and thin filaments (Fig. 7B,C) when compared with *Myo18B*$^{+/+}$ cardiac myocytes (Fig. 7A). Additionally, in transverse sections of myofibrils, *Myo18B*$^{+/+}$ myocytes showed ordered alignment of thick filaments and of thin filaments surrounding thick filaments (Fig. 7D,D′); however, *Myo18B*$^{-/-}$ myocytes showed disordered alignment and unbalanced distribution of thick and thin filaments (Fig. 7E,E′,F,F′). These data indicate that Myo18B is necessary for the development and/or maintenance of normal cardiac myofibril structure.